BEAM-BEAM EFFECTS IN CEPC AND TLEP

Kazuhito Ohmi, KEK

Abstract

Higgs particles are discovered in LHC at the mass of 126 GeV. The mass is in possible range for circular Higgs factory. Two proposals for high energy electron positron colliders are being submitted from Europe and China. The colliders are called TLEP and CEPC, respectively. It was considered that very high energy lepton colliders are inefficient for two reasons; high beam power loss and strong beamstrahlung in the beam-beam interaction. We discuss the beamstrahlung in two colliders theoretical and simulations.

INTRODUCTION

Studying the beam-beam effects is essential to determine the beam parameters in colliders. In Higgs factories, beamstrahlung, which is synchrotron radiation emitted by beam-beam collision, seriously affects the bunch length. To get high luminosity $L \sim 10^{34}$ cm^{-2}s^{-1}, vertical beta function at the interaction point (IP) is squeezed strongly, since the successes and ongoing project of B factories, PEP-II, KEKB and SuperKEKB. The bunch lengthening may break hourglass condition $\beta_y > \sigma_z$. The design parameter should be determined with taking into account the bunch lengthening. The colliders, PEP-II and KEKB, have operated with the condition $\beta_y \leq \sigma_z$. Simulations of beam-beam interaction have worked as powerful tool for optimization of the operating condition. For Higgs factories, highly qualitative design based on the simulations can be made possible. Table 1 shows the parameters of CEPC and TLEP.

Beamstrahlung is inevitable subject in very high energy e+e- circular colliders [1, 3]. Energy of photon emitted by beam-beam force, which is called beamstrahlung, is much harder than that of bending magnet, because of orbit radius is smaller than the bending radius. High relativistic factor γ shift photon energy higher. We discuss beam-beam interaction with considering beamstrahlung as a key subject.

BEAMSTRAHLUNG

Beamstrahlung is synchrotron radiation emitted during the beam-beam interaction. The curvature of beam orbit during the beam-beam interaction is far smaller than that of bending magnets. Energy of emitted photon during the interaction is very high and the number is less than one per collision. Energy spread of the beam is damaged by the emission, which is hard and stochastic.

We first sketch the beamstrahlung using analytic formulae. Linearized Beam-beam force is written as follows,

$$(\Delta p_x, \Delta p_y) = \frac{2N_e r_e}{\gamma} \frac{1}{\sigma_x + \sigma_y} \left(\frac{x}{\sigma_x}, \frac{y}{\sigma_y} \right). \quad (1)$$

where N_e is the bunch population, r_e the classical electron radius, and $\sigma_{x/y}$ is horizontal/vertical beam size at IP. $p_{x,y}$, which is normalized by total momentum p_0, is $(1+\delta)dx/ds$, where $\delta = \Delta E/E_0$ is energy deviation for the design beam energy. Substituting $x = \sigma_x$ and $y = \sigma_y$ as typically numbers, the momentum change is expressed by

$$\Delta p_{xy} = \frac{2N_e r_e}{\gamma(\sigma_x + \sigma_y)} \quad (2)$$

The beam-beam force acts during the interaction $\Delta s = \sqrt{\pi/2}\sigma_z$, where it is notified that the colliding beam also moving light speed. The curvature of a beam particle is expressed by

$$\frac{1}{\rho} \approx \frac{\Delta p_{xy}}{\Delta s} = \frac{2Nr_e}{\sqrt{\pi/2}\gamma\sigma_x\sigma_z}. \quad (3)$$

The orbit radii are 23.3 and 38.7 m for CEPC and TLEP-H, respectively. While the radii of bending magnets are 6,094 and 11,000 m, respectively. The radii during the beam-beam interaction are far smaller than those of bending magnets.

The synchrotron radiation is emitted by the beam particles moving with curvature $1/\rho = \sqrt{1/\rho_x^2 + 1/\rho_y^2}$. Characteristic energy of the synchrotron radiation is expressed by

$$u_c = \hbar\omega_c = \frac{3\hbar c\gamma^3}{2\rho}. \quad (4)$$

The energies are 0.16 and 0.099 GeV for CEPC and TLEP-H, respectively. The energies is far less than the beam energy, $E_0 = 120$ GeV.

Spectrum of the synchrotron radiation is expressed using K Bessel function

$$\frac{dn_\gamma(\omega)}{d\omega} = \frac{\sqrt{3}\alpha\gamma\Delta s}{2\pi\rho\omega_c} S(\omega/\omega_c) \quad (5)$$

where

$$S(\xi) = \int_\xi^\infty K_{5/3}(y)dy. \quad (6)$$

K is K-Bessel function and $\alpha = e^2/4\pi\epsilon_0\hbar c \approx 1/137$ is the fine structure constant.

ISBN 978-3-95450-172-4

Table 1: Parameter Table of Higgs Factories

	CEPC	TLEP-H	TLEP-t	unit
circumference	53.6	100	100	km
energy	120	120	175	GeV
bunch population	3.71	0.46	1.4	$\times 10^{11}$
emittance $\varepsilon_{x/y}$	6.8/20	0.94/1.9	2/2	nm/pm
$\beta^*_{x/y}$	800/1.2	500/1	1000/1	mm
damping time $\tau_{xy/z}/T_0$	79.70/39.85	144/72	46/23	turns
natural bunch length	2.26	0.81	1.16	mm
natural energy spread	0.13	0.10	0.14	%
synchrotron tune	0.206	0.096	0.10	
number of bunches	50	1360	98	
number of IP	2	4	4	
luminosity	1.82	6.0	1.8	10^{34} cm^{-2}s^{-1}/IP
Beamstrahlung				
bunch length	2.58	1.17	1.49	mm
energy spread	0.15	0.14	0.19	%

Number of emitted photon is obtained by integrating over ω.

$$n_\gamma = \int_0^\infty \frac{dn_\gamma(\omega)}{d\omega} d\omega = \frac{5\sqrt{3}\alpha\gamma}{6\rho}\Delta s \tag{7}$$

The number of photon emitted by the radiation is expressed by the beam parameters in Eq.(2)

$$n_\gamma = \frac{5}{\sqrt{3}}\frac{\alpha N_e r_e}{\sigma_x + \sigma_y}. \tag{8}$$

Actually ρ varies along s and depends on x, y due to the nonlinear beam-beam force. Taking into account of the variations, the number of photon is given by [2, 3]

$$n_\gamma = 2.12\frac{\alpha r_e N_e}{\sigma_x + \sigma_y}, \tag{9}$$

Averaged energy of emitted photon is given by integral of the power spectrum as follows,

$$\langle u \rangle = \frac{3}{5\pi}\hbar\omega_c \int_0^\infty \xi S(\xi) d\xi = \frac{8}{15\sqrt{3}}\hbar\omega_c. \tag{10}$$

Multiplying the number of photon, averaged energy loss of a beam particle is obtained as follows,

$$\langle \Delta E \rangle = n_\gamma \langle u \rangle \Delta s = \frac{2\hbar\alpha c\gamma^4}{3\rho^2}. \tag{11}$$

The energy loss is expressed using accelerator parameters as

$$\frac{\langle \Delta E \rangle}{E_0} = \frac{16\sqrt{\pi/2}}{3\pi} r_e^3 \gamma \left(\frac{N_e}{\sigma_z(\sigma_x + \sigma_y)}\right) \sigma_z. \tag{12}$$

Considering trajectory dependence again, the averaged energy loss is given by [2, 3],

$$\langle d\delta_{BS} \rangle = \frac{\langle \Delta E \rangle}{E_0} = 0.864 r_e^3 \gamma \left(\frac{N_e}{\sigma_z(\sigma_x + \sigma_y)}\right)^2 \sigma_z. \tag{13}$$

The square average of photon energy is given by [4]

$$\langle u^2 \rangle = \frac{3}{5\pi}(\hbar\omega_c)^2 \int_0^\infty \xi^2 S(\xi) d\xi = \frac{11}{27}(\hbar\omega_c)^2. \tag{14}$$

The diffusion of beam energy due to the square average is given by

$$n_\gamma \langle u^2 \rangle = \frac{55}{24\sqrt{3}} \frac{r_e \hbar m c^3 \gamma^7}{\rho^3} \Delta s. \tag{15}$$

The contribution to the energy spread is expressed by

$$\frac{\langle \Delta E^2 \rangle}{E_0^2} = \frac{n_\gamma \langle u^2 \rangle}{E_0^2} = n_\gamma \frac{11}{27}(\hbar\omega_c)^2 = \frac{275}{64 n_\gamma}\left(\frac{\langle \Delta E \rangle}{E_0}\right)^2 \tag{16}$$

The other diffusion source is randomness of n_γ, which is less than 1. The quantum effect had been studied in Ref.[2, 3] The deviation of the energy loss is given for round Gaussian beam as

$$\sqrt{\langle d\delta_{BS}^2 \rangle} = \langle d\delta_{BS} \rangle \sqrt{0.1639 + \frac{5.129}{n_\gamma}}. \tag{17}$$

That for flat Gaussian beam is given by

$$\sqrt{\langle d\delta_{BS}^2 \rangle} = \langle d\delta_{BS} \rangle \sqrt{0.333 + \frac{4.583}{n_\gamma}}. \tag{18}$$

The diffusion is accumulated during the radiation damping time and equilibrium energy spread is realized. Equilibrium energy spread for radiation damping and beamstrahlung is given by

$$\sigma_{\delta,BS} = \frac{1}{2}\sqrt{\tau_z N_{IP}} \sqrt{\langle d\delta_{BS}^2 \rangle}, \tag{19}$$

ISBN 978-3-95450-172-4

Table 2: Parameters Concerning Beamstrahlung

	CEPC	TLEP-H	TLEP-t	unit
γ	2.35	2.35	3.42	10^5
ρ	23.3	38.7	88.6	m
u_c	0.16	0.099	0.13	GeV
n_γ	0.21	0.092	0.13	

where τ_z is the longitudinal radiation damping time in the unit of turn. Taking into account of energy spread due to the synchrotron radiation, total energy spread is given by

$$\sigma_{\delta,tot} = \sqrt{\sigma_{\delta,SR}^2 + \sigma_{\delta,BS}^2}. \quad (20)$$

Enlargement of energy spread induces bunch lengthening, $\sigma_{z,tot} = \sigma_{z,SR}\sigma_{\delta,tot}/\sigma_{\delta,SR}$. The lengthening makes relax the beamstrahlung. Therefore the bunch length and energy spread are solved self-consistently.

Parameters related to beamstrahlung for CEPC and TLEP are summarized in Table 2.

Simulation of Beamstrahlung

Figure 1 sketches the simulation scheme of the beamstrahlung during beam-beam interaction. A beam particle (red line) passes through a bunch (blue ellipse), which is sliced several into pieces. Trajectory of the particle is calculated slice-by-slice by using Bassetti-Erskine formula [5] or Poisson solver based on Particle In Cell method[6]. The bunch is sliced into 20 pieces for the simulations presented in this paper. Synchrotron radiation is emitted by the interaction of slices with the probability of Eq.(7). Both beams move with the light speed. The traveling distance of particles between interactions with i-th and (i+1)-th slices is expressed by

$$ds = \frac{z_i - z_{i+1}}{2}. \quad (21)$$

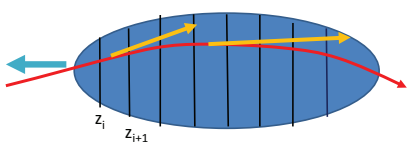

Figure 1: Simulation scheme of the beamstrahlung during beam-beam interaction.

Two types of beam diffusion are examined and compared in this paper.

Gaussian excitation model Photon is generated by the probability n_γ in Eq.(7). The average energy and square average are given Eqs.(10) and (14). The deviation of the photon energy is expressed by

$$\langle u^2 \rangle - \langle u \rangle^2 = \frac{211}{675}(\hbar\omega_c)^2. \quad (22)$$

Beamstrahlung, energy loss of the beam particle, is evaluated by the photon emission with the energy, which is generated by Gaussian random numbers with the average energy in Eq.(10) and the deviation in Eq.(22).

Realistic radiation Photon is generated by the probability n_γ in Eq.(7) again. The photon higher than $\hbar\omega$ is generated by the probability as follows,

$$\mathcal{N}_\gamma(\omega) = \frac{3}{5\pi}\int_{\omega/\omega_c}^{\infty} S(\xi)d\xi \quad (23)$$

where $\mathcal{N}_\gamma(0) = 1$ and $\mathcal{N}_\gamma(\infty) = 0$. The energy of emitted photon is determined by the inverse of $\mathcal{N}$,

$$\omega = \mathcal{N}_\gamma^{-1}(\hat{r}) \quad (24)$$

where $\hat{r}$ is uniform random number $0 < \hat{r} < 1$. Figure 2 shows $\mathcal{N}_\gamma(\omega)$.

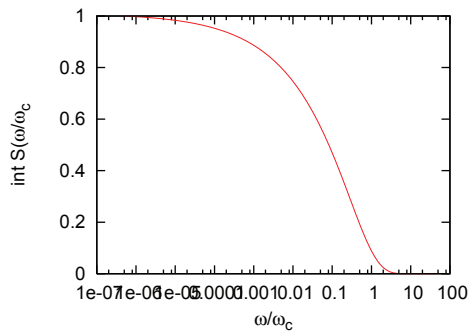

Figure 2: Plot of $\mathcal{N}_\gamma(\xi)$.

EVOLUTION BEAM ENERGY DISTRIBUTION DUE TO BEAMSTRAHLUNG

Photon energy spectrum is obtained so that macroparticles (10^7) collide with Gaussian beam with the design parameters (natural beam sizes determined by synchrotron radiation). Figure 3 shows energy spectrum of the emitted photon. The number of photon emission is 20% of the beam particle ($n_\gamma = 0.2$) for single collision in CEPC (Table 2). The line shown in the figure draw $S(\xi)$, where $u_c = 0.13$ GeV is slightly smaller than the analytical estimate using Eq.(4) and (3), $u_c = 0.16$ GeV. The blue line in the figure is Gaussian distribution using $\langle u^2 \rangle$ in Eq.(10), $0.2N_e(2\pi\langle v^2\rangle)^{-1/2}\exp(-v^2/2\langle v^2\rangle)dv$, where $v \equiv u/E_0$. The tail of energy distribution remarkably spreads higher energy side for K Bessel formula compare than Gaussian. Needless to say, the spectrum of $S(\xi)$ and Gaussian give the same square average $\langle u^2 \rangle$. When n_γ is large and characteristic energy (u_c) is much smaller than the beam energy like radiation of bending magnet, the tail of energy distribution is not observable in equilibrium distribution. For beamstrahlung in very high energy colliders, n_γ is small and u_c is large.

ISBN 978-3-95450-172-4

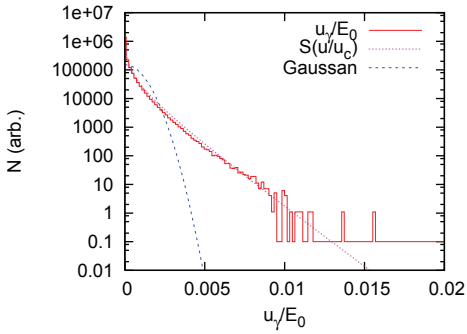

Figure 3: Energy spectrum of emitted photon.

We next focus on evolution of beam energy distribution, in which two beams with the design natural bunch length and energy spread start collision. Figure 4 shows turn-by-turn change of the energy distribution due to the beamstrahlung. Pictures (a) and (b) show evolutions of the energy distribution without and with synchrotron motion, respectively. Each line shows the distribution after beam-beam collisions, whose number is marked in the figure. The macro-particle number is 10^7. The energy distribution spreads negative direction (loss) for the absence of synchrotron motion. Though the tail is accumulated, the number is not large, several 10 lower then -$10\sigma_\delta = 0.13\%$ of the total energy. When synchrotron motion is taken into account, the tail appear in both side, $\sim \pm 10\sigma_\delta$. The number of particles out of $\pm 10\sigma_\delta$ are less. The beam loss just after injection does not seem serious.

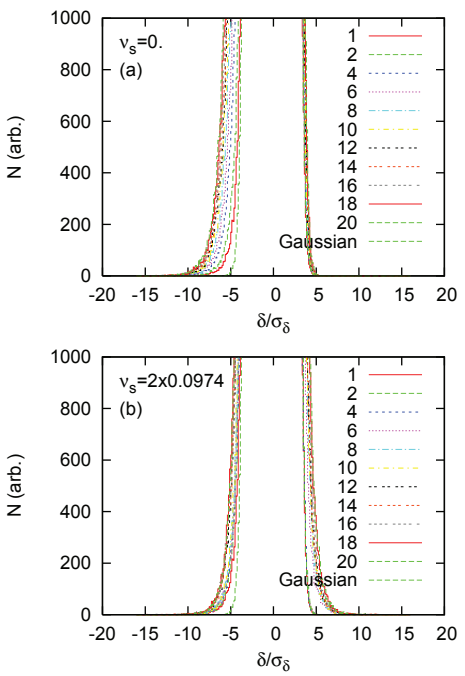

Figure 4: Energy spread change. Pictures (a) and (b) show evolutions of the energy distribution without and with synchrotron motion, respectively.

Figure 5 shows equilibrium distribution of the energy spread. Energy and longitudinal distributions. In the whole distribution of z and δ, those of K Bessel excitations is not distinguished from those with Gaussian. The difference is clear in the tail distribution of the right two pictures.

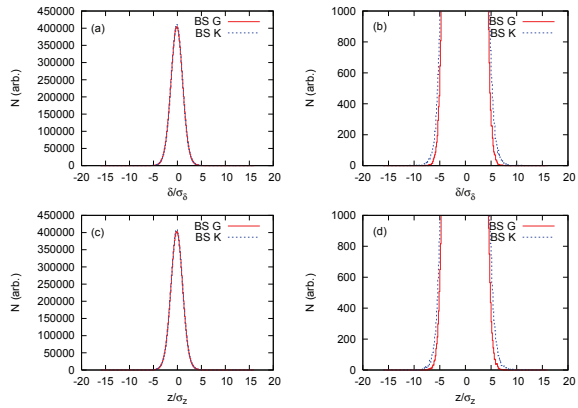

Figure 5: Equilibrium distribution of the energy deviation and z. Pictures (a) and (b) are whole and tail distribution in z, respectively. Pictures (c) and (d) are for the energy deviation δ.

LUMINOSITY EVALUATION USING SIMULATION

Luminosity is evaluated by the weak-strong and strong-strong simulations, which include beamstrahlung treated in previous section.Beamstrahlung causes the energy spreading, which results bunch lengthening. We assume the intensity of both beam is the same, thus bunch length due to beamstrahlung is also the same. The bunch length of the weak beam is calculated turn-by-turn, and is taken average in average 100-1000 turns. The bunch length of the strong beam is revised every 100-1000 turns. The bunch length in the weak-strong simulation is revised self-consistently every 100-1000 turns. The bunch length is calculated turn-by-turn in the strong-strong simulation.

Figure 6 shows evolutions of luminosity and beam sizes $\sigma_x, \sigma_y, \sigma_z$ for CEPC. Three lines are drawn in the figure; red, blue, and green correspond to Gaussian, K Bessel and none for beamstrahlung, respectively. The radiation damping time is 80 turns in transverse, thus the simulation is performed during 12 radiation damping time (1000 turns). Beamstrahlung causes bunch lengthening, which results vertical beam size blowup and luminosity degradation. There is no difference in luminosity and beam sizes between Gaussian and K Bessel for beamstrahlung.

The simulation was done for several bunch populations, 0.6×, 0.8×, 1×,1.2× of the design population, $N_e = 3.71 \times 10^{11}$. Figure 7 shows luminosity and beam sizes as function of bunch population. The horizontal size decreases for increasing bunch population due to dynamic beta $\nu_x/IP = 0.54$. Other parameters, luminosity, σ_y and

ISBN 978-3-95450-172-4

σ_z, increase for higher bunch population. Luminosity does not increase quadratically, since the increases of σ_y and σ_z.

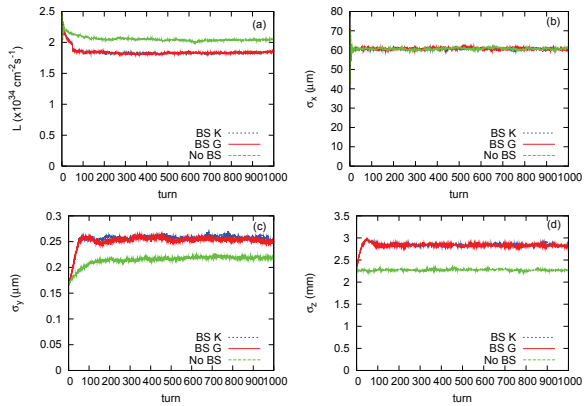

Figure 6: Luminosity and beam sizes for CEPC in a weak-strong simulation (BBWS).

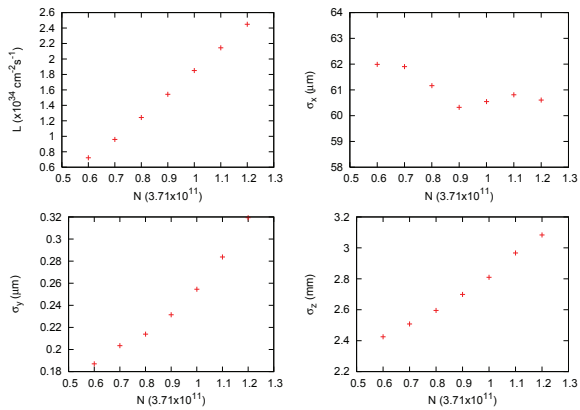

Figure 7: Luminosity and beam sizes depending on the bunch populations for CEPC in a weak-strong simulation using BBWS.

Luminosity and beam sizes are also evaluated by a strong-strong simulation using a code "BBSS"[6]. Figure 8 shows evolution of luminosity and beam sizes, $\sigma_x, \sigma_y, \sigma_z$. Luminosity evolution of three tune operating points are depicted in plot (a). Depending on tune (0.54,0.58), luminosity is unstable. The tune is factional part of IP to IP, the total fractional tune is twice for CEPC. Plots (b)-(d) show evolution of the beam sizes for stable (0.54,0.61) and unstable (0.54,0.58) cases. In unstable case, vertical beam sizes of both beams increase correctively. We use the operating point (0.54,0.61) hereafter [7, 8].

The simulation is performed for several vertical beta function at IP, $\beta_y^* = 1.2$ (design),2,3,4, and 5 mm. Figure 9 shows geometrical beam-beam tune shift and luminosity as function of β_y^*. Geometrical and simulated luminosities are plotted by blue and red points, respectively, in the plot (b), where "geometrical" means beam-beam parameter and luminosity calculated by design bunch shape. The hourglass effect and bunch lengthening due to beamstrahlung is taken into account in the tune shift. The tune shift is monotonically increases for β_y^*, but is not linear. Geometrical and simulated luminosity by BBSS are plotted. Geometrical luminosity decreases for higher β_y^*. The simulation shows mild decrease compare than geometrical one. This behavior is due to dynamic beta and beam-beam limit under hourglass effect.

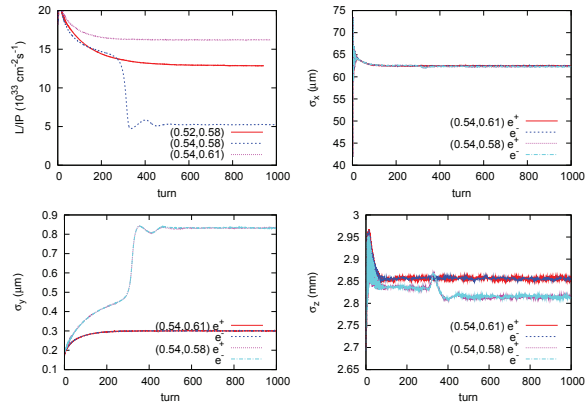

Figure 8: Luminosity and beam sizes in CEPC calculated by a strong-strong simulation (BBSS).

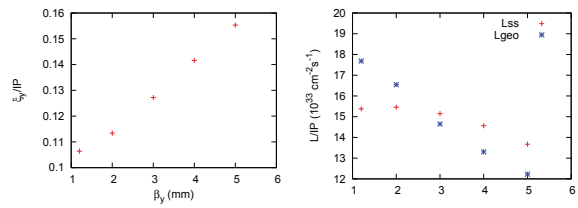

Figure 9: Geometrical beam-beam tune shift and luminosity as function of β_y^*. Geometrical and simulated luminosities are plotted by blue and red points, respectively, in the plot (b).

In a real operation of an accelerator, beam current of one beam sometimes is lost considerable amount. The accelerator is expected to be operated stably under the occasion. Figure 10 shows evolution of the luminosity and beam sizes for current asymmetry, where one beam (electron beam in this case) has a half intensity of the design. Luminosity degrades one third (not half) and vertical size and bunch length of electron beam increase. The bunch length of positron beam is going toward the design value. The lifetime of the weak(e^-)-beam is discussed in next section.

Figure 11 shows tolerance of luminosity for vertical dispersion. The luminosity degrades for $\eta_y = 0.02 - 0.05$ mm clearly. This result is requirement for IP optics correction.

Table 3 summarizes luminosity given by the simulations for CEPC and TLEP[9].

ISBN 978-3-95450-172-4

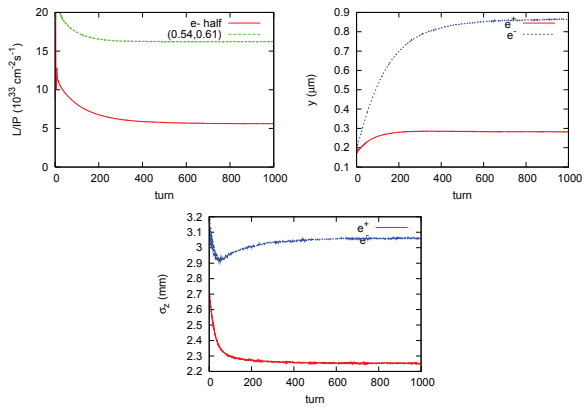

Figure 10: Luminosity and beam sizes for current asymmetry in CEPC calculated by a strong-strong simulation (BBSS).

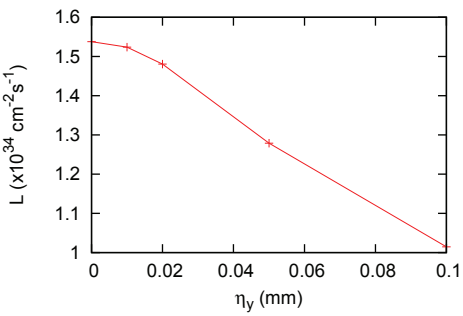

Figure 11: Luminosity as function of vertical dispersion calculated by a strong-strong simulation (BBSS).

Table 3: Calculated Luminosity and Bunch Length[9]

	TLEP/FCC-ee					Ce-
	Z	Z (cr. w.)	W	t	H	pC
	luminosity [10^{34} cm^{-2}s^{-1}]					
analyt.	28	219	12	6.0	1.7	1.8
w-s.	21	150	13	6.9	2.0	1.6
s-strong	—	—	—	7.5	2.2	1.6
	σ_z [mm]					
w/o BS	1.64	1.9	1.01	0.81	1.16	2.3
analyt.	2.56	6.4	1.49	1.17	1.49	2.7
w-s.	2.8	7.9	1.5	1.2	1.6	2.7
s-strong	—	—	—	1.3	1.72	2.9

LIFETIME EVALUATION

Beam lifetime is evaluated by the equilibrium distribution. In the equilibrium, outgoing flow due to diffusion from an aperture is equal to damping flow due to damping[4]. The damping flow is continuously and easily estimated. Another method for the lifetime evaluation is direct simulation, in which number of particle outgoing the aperture is counted.

We consider equilibrium distribution $f(J_i)$ expressed by J_i. J_i is constant for betatron/synchrotron oscillation. The incident flow at an aperture $J_{i.max}$ for time step dt is given by multiplication of the density at $J_{i,max}$ and damping of J_i in dt,

$$\frac{dN}{dt} = f(J_i)\frac{dJ_i}{dt} \tag{25}$$

The radiation damping time is given by

$$\frac{dJ_i}{dt} = -\frac{2J_i}{\tau_i} \tag{26}$$

The assumption, in which outgoing flow is the same as incident flow, means that the beam lifetime (τ_ℓ) is given by

$$\tau_\ell = \frac{N}{\frac{dN}{dt}} = \frac{t_i}{2J_{i,max}f(J_{i,max})} \tag{27}$$

For example of Gaussian distribution, $f(J_i) = \varepsilon_i^{-1}\exp(-J_i/\varepsilon_i)$, the lifetime, which is popular formula, is given by

$$\tau_\ell = \frac{\tau_i}{2}\frac{\varepsilon_i}{J_{i,max}}\exp(J_{i,max}/\varepsilon_i) \tag{28}$$

where $J_{i,max} = \beta_i x_{max}^2$.

Figure 12 shows beam tail distribution $g(r_i)$ in x, y, z directions. The distributions for bunch populations, $(0.6, 0.8, 1.0, 1.2) \times 3.71 \times 10^{11}$ are drawn. The horizontal axes is $r_i = \sqrt{2J_i/\varepsilon_i}$. The lifetime formula is written as

$$\tau_\ell = \frac{\tau_i dr_i}{r_{i,max}g(r_{i,max})dr_i} \tag{29}$$

where $r_{z(y),max} = z(y)_{max}/\sigma_{z(y)}$. Figure 13 shows the lifetime for aperture $r_{i,max}$ in each bunch population. Lifetime limited by horizontal aperture is not plotted, since the horizontal distribution does not have long tail.

We discuss the beam halo and lifetime, when one beam is lost to a half intensity. The beam sizes of the strong beam (without loss) approach to the design values, while those of the weak beam (with loss) blow up. Figure 14 shows the tail distributions of z and y, and related life times. It may be hard to keep the beam, once a loss starts.

Figure 15 shows Luminosity and lifetime dependence on the natural bunch length.

The same simulations are performed for TLEP. Figure 16 and 17 shows tail distributions and lifetime for TLEP. Figure 18 shows results of beam loss simulation with the aperture limit of $\delta_{max} = 1.5\%$. The lifetime is 26 min

ISBN 978-3-95450-172-4

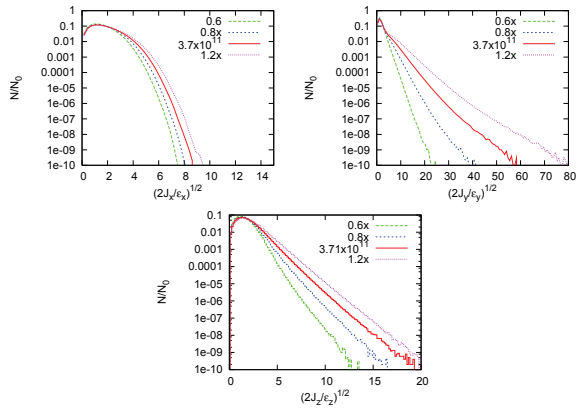

Figure 12: Beam halo distribution in CEPC.

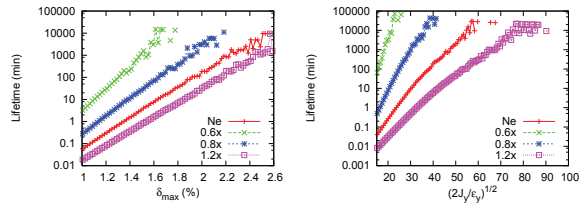

Figure 13: Beam lifetime due to energy and vertical aperture for CEPC.

(H) and 0.31 min (t). The lifetime estimated by the damping flow in Figure 17 agree with that given by the beam loss simulation.

The lifetime is evaluated by analytical formulae [3, 10]. Simulations [10, 11] including results in this paper have shown shorter lifetime than the formulae. Taking into account of the dynamic beta, the formulae gave similar lifetime as these simulations [12].

CONCLUSIONS

Gaussian and realistic K Bessel beamstrahlung excitation have been examined. Longitudinal beam tail due to beamstrahlung is enhanced. It is essential for lifetime. No difference between Gauss and K Bessel excitations in luminosity and core beam sizes in the both of weak-strong and strong-strong simulations. Strong-strong simulation, (0.54,0.61) is a nice operating point. [7]. Luminosity simulation can be done using effective bunch length and energy spread for beamstrahlung in usual beam-beam codes.

Dependence on luminosity for $\beta_y^* = 1.2-3$ mm is weak. $\beta_y^* = 2$ mm may be a good solution. Tolerance for vertical dispersion, $\eta_y^* < 0.05$ mm. For asymmetric beam, an equilibrium state exists. Lifetime of weak beam should be cared. Long term tracking containing beamstrahlung has been done using weak strong simulation. Beam lifetime was evaluated by the longitudinal and transverse distributions. The lifetime estimated by the damping flow agree with the beam loss simulations. $\delta_{max} > 1.8\%$ (100 min) is required for CEPC. y_{max}/σ_y¿40 (100 min) is required in transverse.

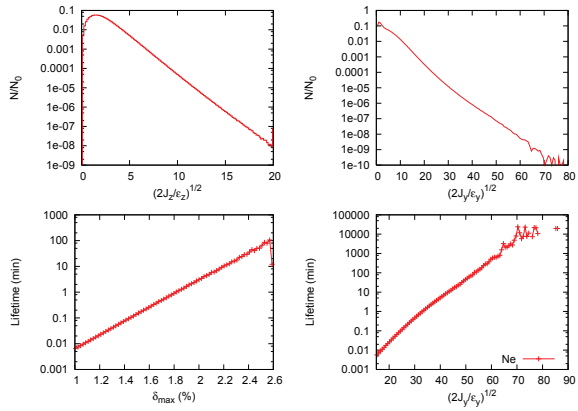

Figure 14: Beam halo distribution and lifetime in CEPC, when one beam is lost to a half intensity.

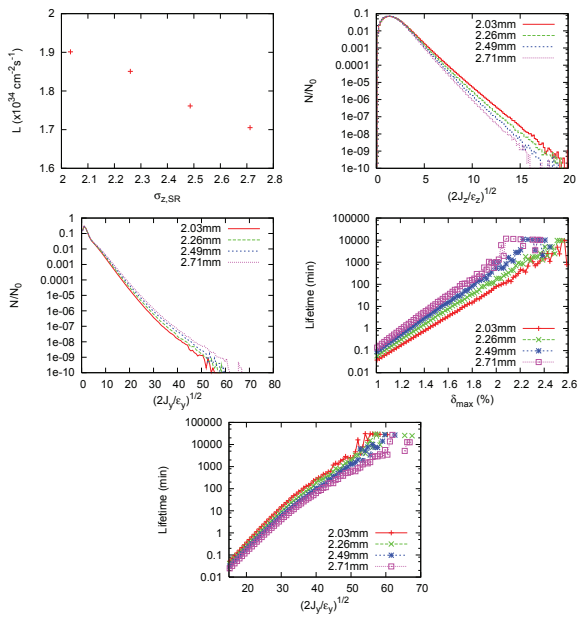

Figure 15: Luminosity and lifetime depending on the natural bunch length.

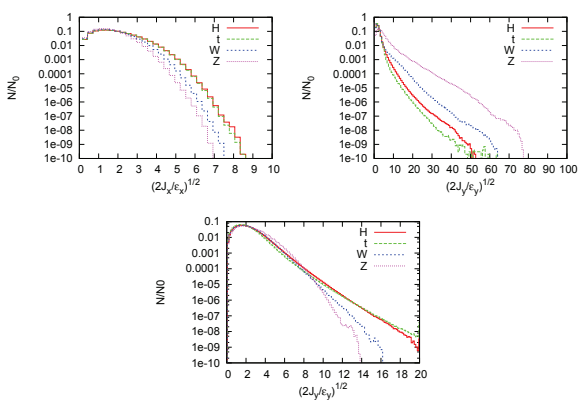

Figure 16: Beam halo distribution in TLEP-H.

ISBN 978-3-95450-172-4

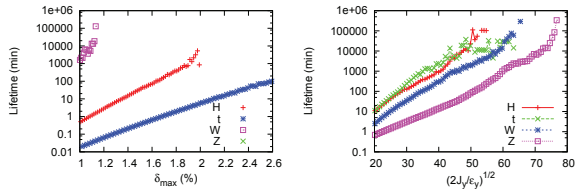

Figure 17: Beam lifetime due to energy and vertical aperture for TLEP.

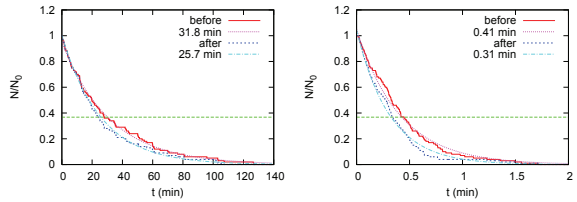

Figure 18: Beam loss in TLEP-H and t.

The author thanks fruitful discussions with W. Chou, M. Koratzinos, D. Shatilov, Y. Zhang, F. Zimmermann.

REFERENCES

[1] K. Yokoya, "Scaling of High-Energy e+e- Ring Colliders," KEK Accelerator Seminar, 15 March 2012.

[2] K. Yokoya, "Quantum Correction To Beamstrahlung Due To The Finite Number Of Photons," Nucl.Instrum.Meth. A251 (1986) 1.

[3] V. Telnov, "Restriction on the energy and Luminosity of e^+e^- Storage Rings due to Beamstrahlung," Phys. Rev. Lett. 110, 114801 (2013).

[4] M. Sands, "The Physics of Electron Storage Rings," SLAC-R-121 (1970).

[5] M. Bassetti and G. Erskine, CERN-ISR TH/80-06 (1980).

[6] K. Ohmi, Phys. Rev. E62, 7287 (2000). K. Ohmi et. al., Phys. Rev. ST-AB 7, 104401 (2004).

[7] D. Shatilov, Y. Zhang, private communications.

[8] Y. Zhang et al.,IPAC14, THPRI003.

[9] K. Ohmi, F. Zimmermann, IPAC14, THPRI004.

[10]A. Bogomyagkov, et al., "Beam-Beam Effects Investigation and Parameter Optimization for Circular e^+e^- Collider TLEP to study the Higgs Boson," PRST-AB 17, 041004 (2014).

[11]S. White and N. Mounet, "Beam-Beam Studies for TLEP (and Update on TMCI)," 6th TLEP workshop, CERN (2013).

[12]M. Koratzinos, in this proceedings.

ISBN 978-3-95450-172-4